Helmstetter et al. (2003)

Mainshocks are aftershocks of conditional foreshocks: How do foreshock statistical properties emerge from aftershock laws

Hugo S. Sánchez-Reyes
ISTerre, Université Grenoble Alpes

Outline

Goal:

What they wanted to answer:

Is it possible to derive most if not all of the observed phenomenology of foreshocks from the knowledge of only the most basic and robust facts of earthquake phenomenology, namely the GR and Omori laws?

They use what is maybe the simplest statistical model of seismicity, the so-called ETAS model (epidemic-type aftershock sequence), based only on the GR and Omori laws.

1. We shall call "foreshock" of type I any event of magnitude smaller than or equal to the magnitude of the following event, then identified as a "mainshock."

2. We shall also consider "foreshock" of type II, as any earthquake preceding a large earthquake, defined as the mainshock, independently of the relative magnitude of the foreshock compared to that of the mainshock.

Inverse Omori law The rate 0 of earthquakes prior to a mainshock increases on average as a power law $\frac{1}{(t_c - t)^{p'}}$

Here, we show that this law results from the direct Omori law for aftershocks describing the power law decay $\sim \frac{1}{(t - t_c)^p}$

Aftershocks of the aftershocks

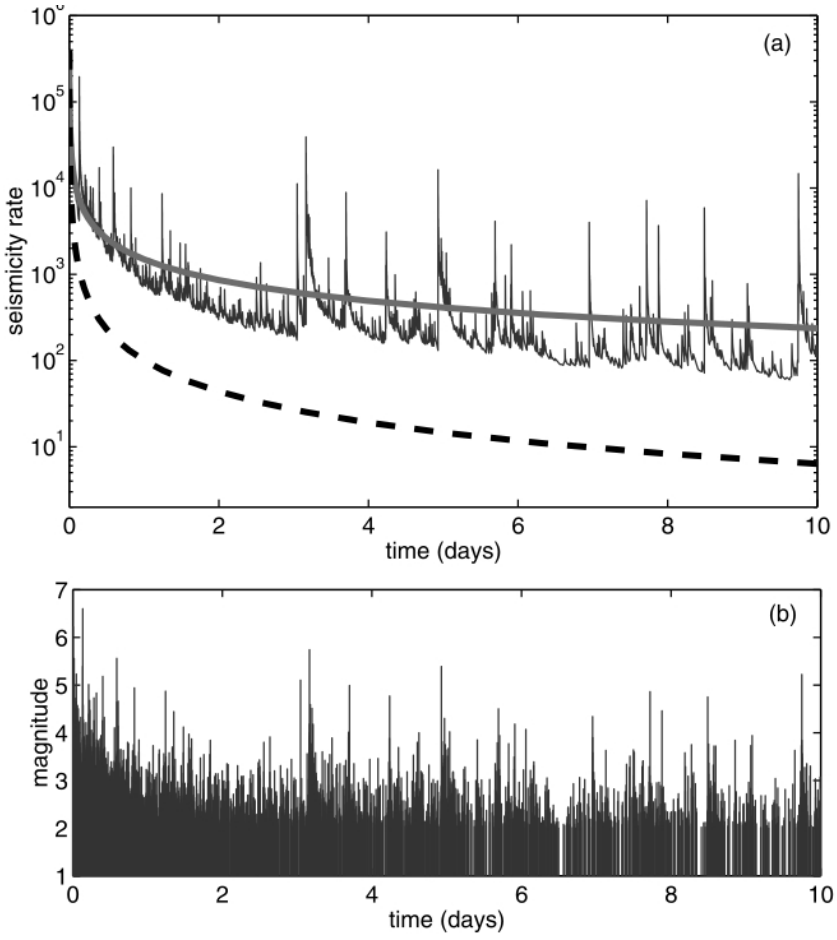

One realization of the ETAS model:
- observed seismicity rate $\kappa(t)$ (noisy solid line)
- average renormalized propagator $K(t)$ (solid line)
- local propagator $\Phi_E(t)$ (dashed line)

The global aftershock rate $\kappa(t)$ is significantly higher than the direct (or first generation) aftershock rate, described by the local propagator $\Phi_E(t)$.

Large fluctuations of the seismicity rate correspond to the occurrence of large aftershocks, which trigger their own aftershock sequence.

Appears the inverse Omori law!

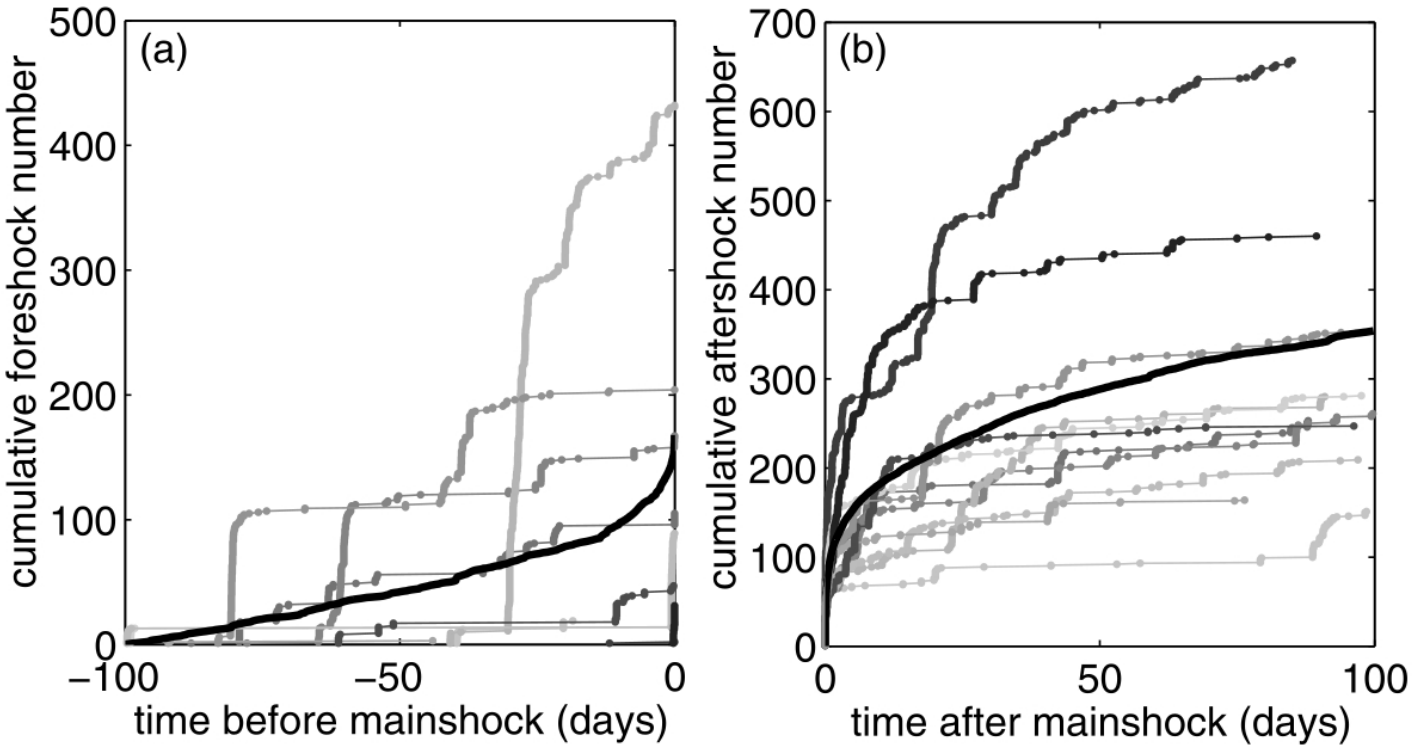

Foreshock (a) and aftershock (b) sequences generated by the ETAS model for $M = 5.5$. The solid black line represents the mean (250seq) seismicity rate before and after a main shock of magnitude $M = 5.5$. Compare to the direct Omori law, clearly observed after any large mainshock, there are large fluctuations from one foreshock sequence to another. The inverse Omori law (accelerating seismicity) is only observed when averaging over a large number of foreshock sequences.

Type II aftershocks are independent of the mainshock energy.

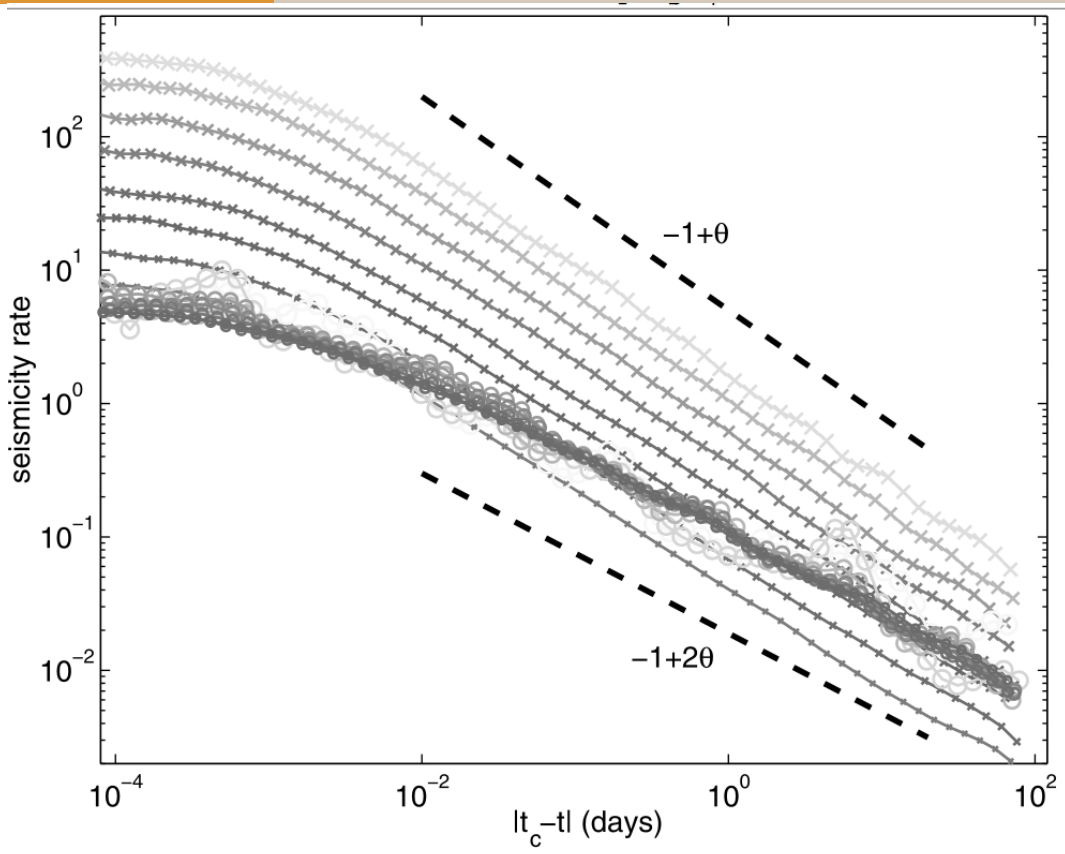

Direct and inverse Omori law for a numerical simulation showing the two exponents $p = 1 - \theta$ for aftershocks and $p' = 1 - 2\theta$ for foreshocks of type II. The rate of aftershocks (crosses) and foreshocks (circles) per main shock, averaged over a large number of sequences, is shown as a function of the time $|t_c - t|$ to the mainshock for different values of the mainshock magnitude [1.5,5]. The number of aftershocks increases with the mainshock energy as $N \simeq E^a$, whereas the number of foreshocks of type II is independent of the main shock energy.

Type II aftershocks are independent of the mainshock energy.

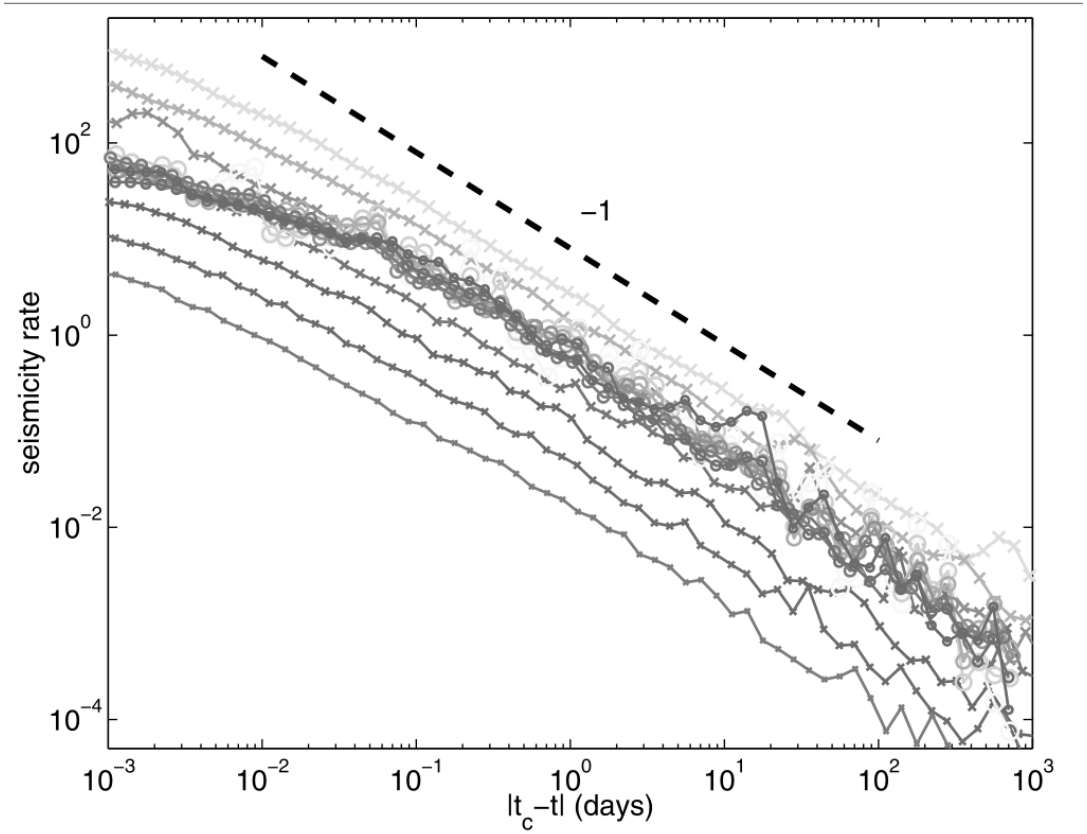

Same as previous, but for $a = 0.8\beta$, showing the larger relative ratio of foreshocks to aftershocks compared to the case a $= 0.5$ b.

When the rate of aftershocks type I and II are close

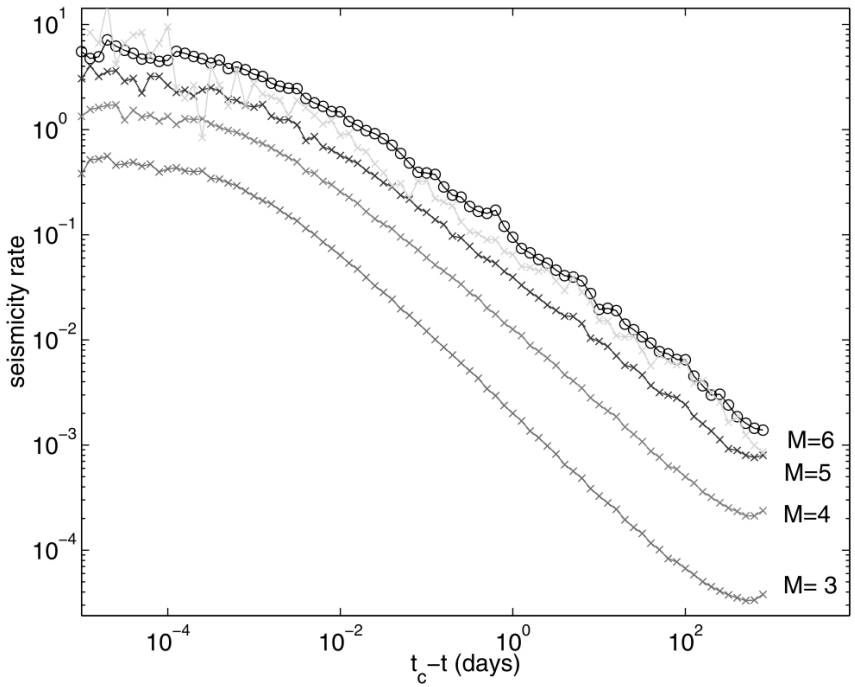

Foreshock seismicity rate per mainshock for foreshocks of type II (circles) and foreshocks of type I (crosses, magnitudes from 3 to 6 of mainshocks) for a numerical simulations. The rate of foreshocks of type II is independent on the mainshock magnitude, while the rate of foreshocks of type I increases with M. For large main shock magnitudes, the rate of foreshocks of type I is very close to that of foreshocks of type II.

p and p' well-predicted when balanced the coupling between the earthquake energies and the seismic rate

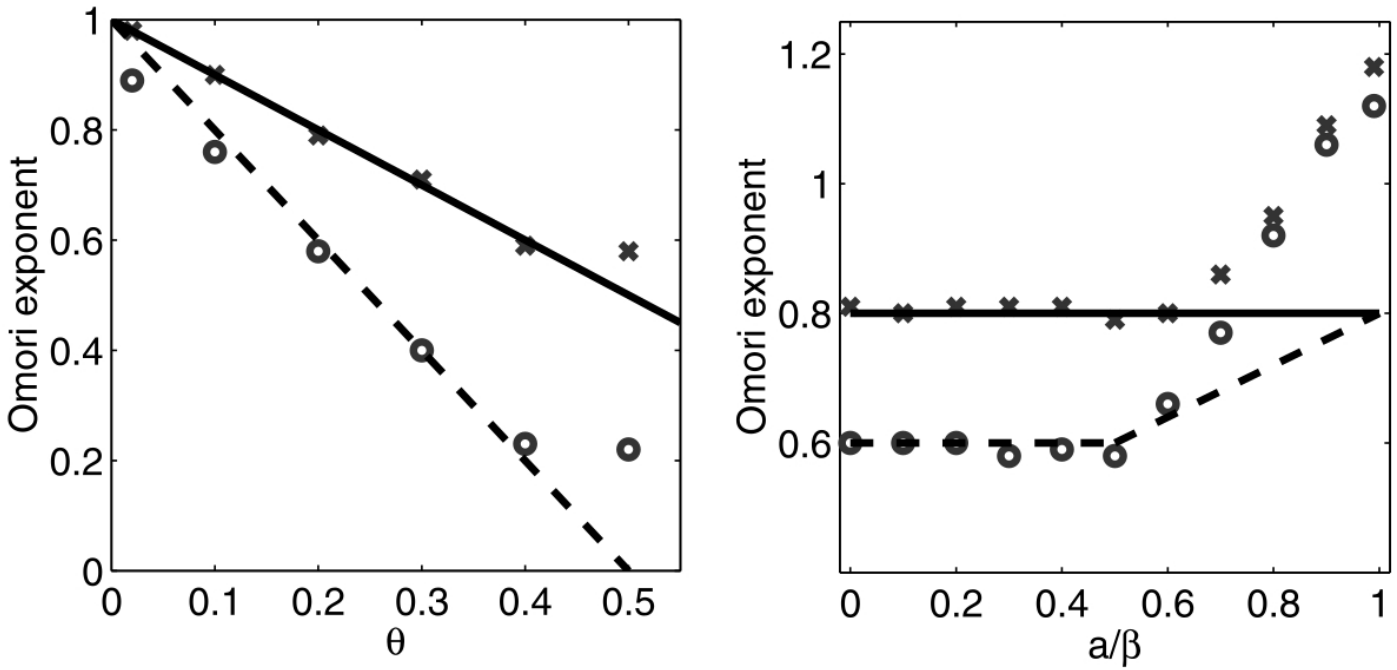

Exponents p and p' of the inverse and direct Omori laws obtained from numerical simulations of the ETAS model. The estimated values of p (circles) for foreshocks and $'$ (crosses) for aftershocks are shown as a function of θ in the case $\alpha = 0.5$ (a) and as a function of α/β in the case $\theta = 0.2$ (b). The theoretical values of p are represented with dashed lines, and the theoretical prediction for p is shown as solid lines.

Magnitude rate as the sum of two power laws!

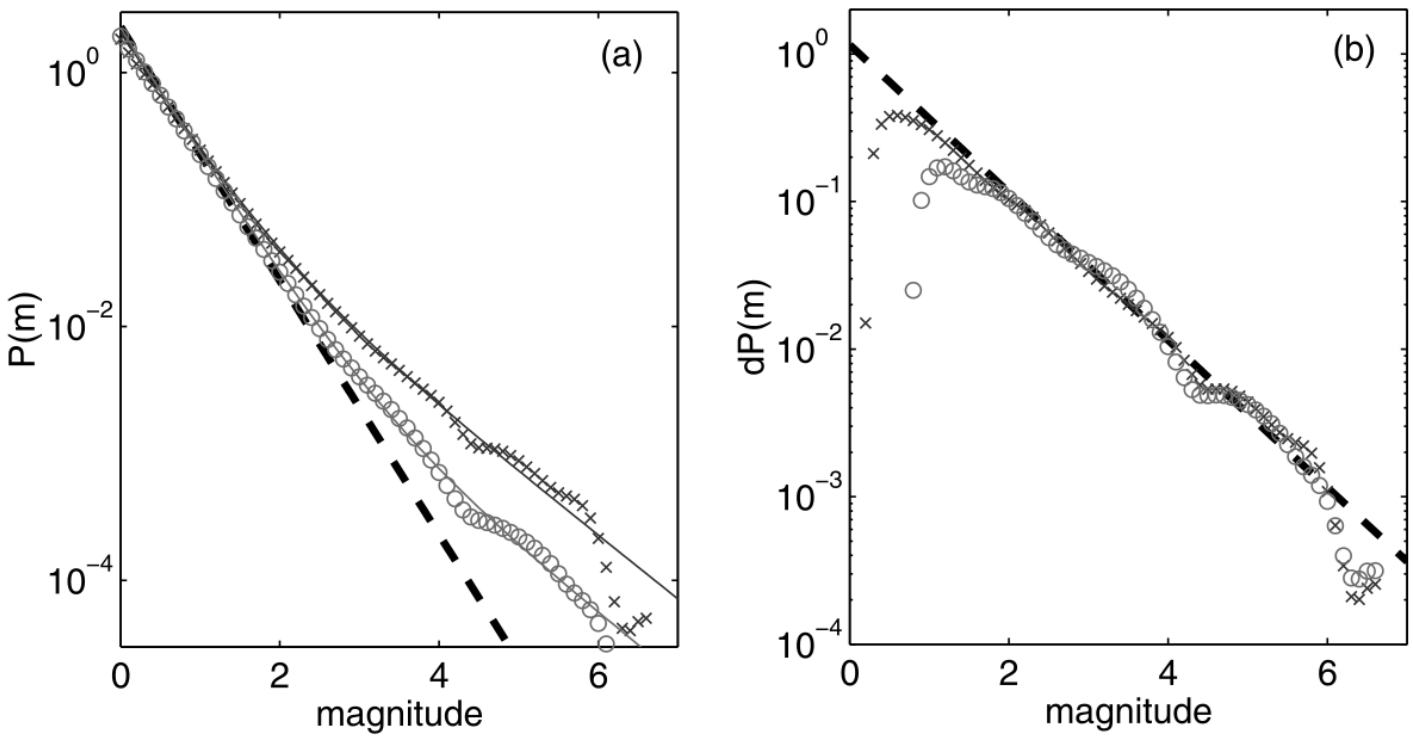

Magnitude distribution of foreshocks for two time periods, $|t_c - t| < 0.1$ days (crosses) and $1 < |t_c - t| < 10$ days (circles), for a numerical simulation of the ETAS model. The solid line for each time period, is the predicted magnitude distribution estimated as the sum of the unconditional GR law with an exponent $b = 1.5\beta = 1$, shown as a dashed black line, and a deviatoric GR law $dP(m)$ with an exponent $b' = b - \alpha = 0.5$ with $\alpha = 1.5a = 0.5$. We must stress that the energy distribution is no more a pure power law close to the mainshock but the **sum of two power laws**.

Magnitude rate as the sum of two power laws!

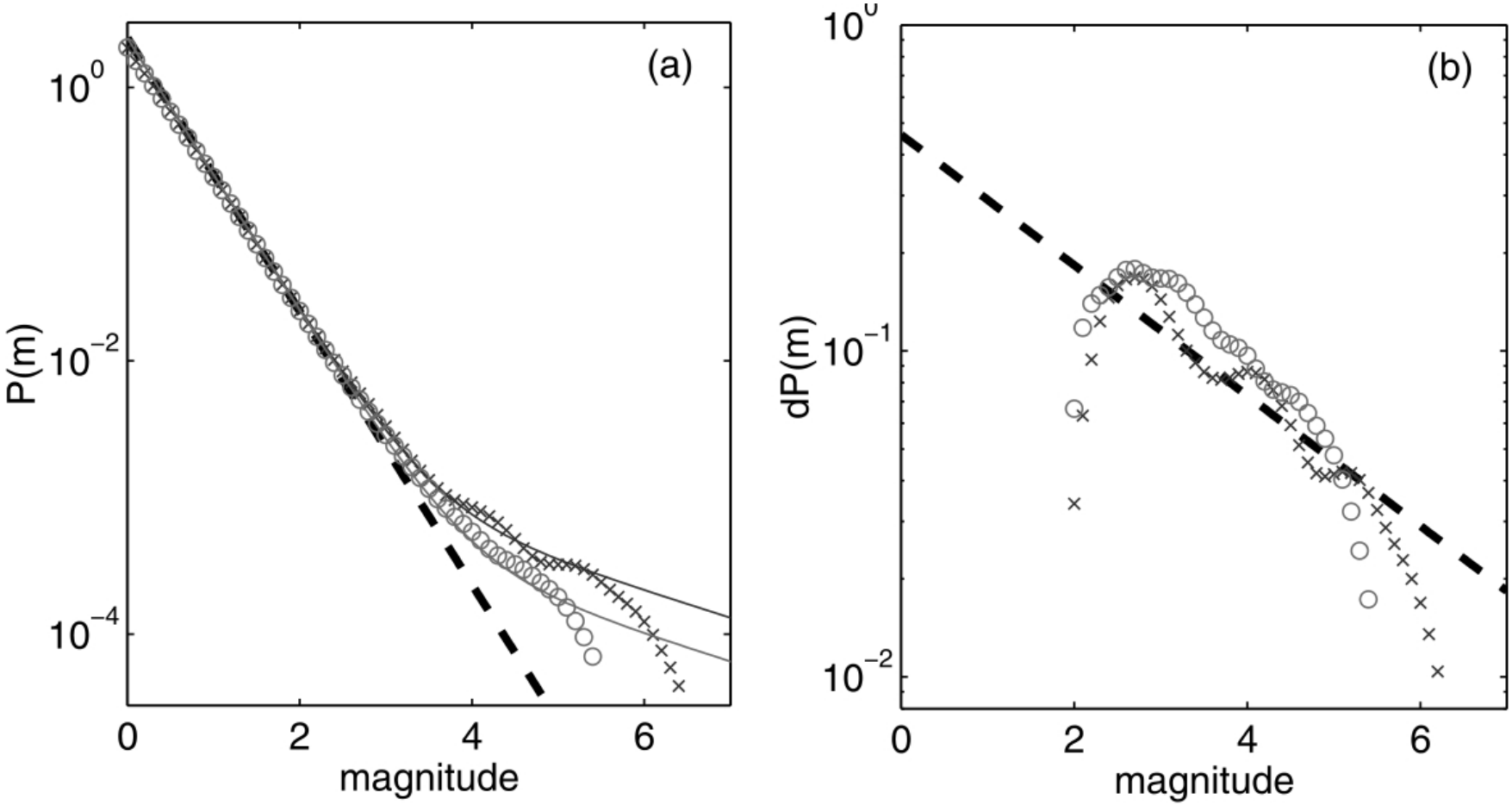

Same as previous, but for $a = 0.8\beta$. In this case, the deviatoric GR contribution is observed only for the largest magnitudes, for which the statistics is the poorest, hence the relatively large fluctuations around the exact theoretical predictions.

Migration of foreshocks as diffusion factor changes

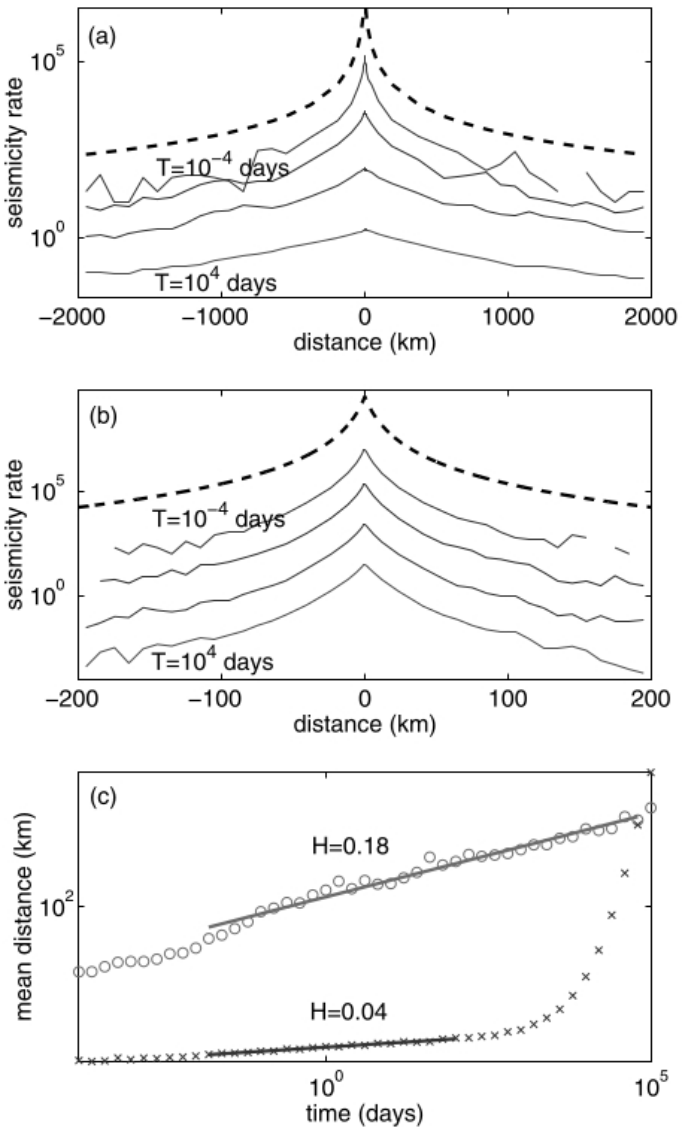

(opposite) Migration of foreshocks for superposed foreshock sequences generated with the ETAS model for two choices of parameters: (a) we see clearly a migration of the seismicity toward the mainshock, larger diffusion exponent H = 0.2. (b) the distribution of the foreshock–mainshock distances shown in panel is independent of the time from the mainshock. Time periods ranging between 10^4 and 10^{-4} days before mainshock. The distribution of mainshock–aftershock distances describing direct lineage is shown as a dashed line. The characteristic size of the foreshock cluster is shown as a function of the time to the mainshock on panel (c) circles correspond to the simulation shown in panel (a) and crosses correspond to the simu-

Seismic rate alarms better than other criteria

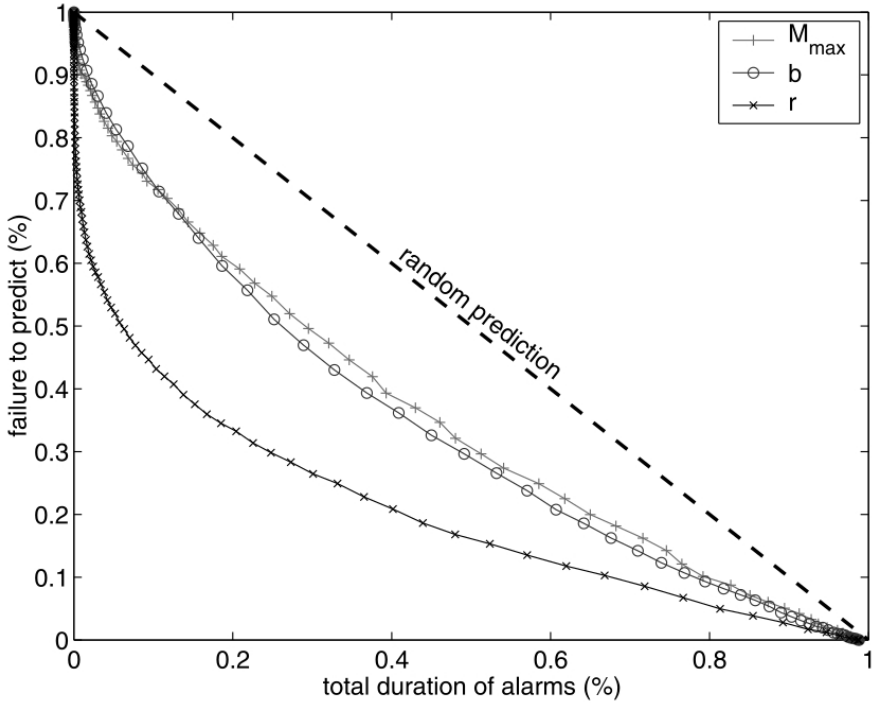

Results of prediction tests for synthetic catalogs. The minimum magnitude is $m_0 = 3$ and the target events are $M > 6$ (a total of 4735 $M > 6$ mainshocks). We use three functions measured in a sliding window of 100 events: (1) the maximum magnitude M max of the 100 events in that window, (2) the apparent GR exponent b measured on these 100 events by the standard Hill maximum likelihood estimator, and (3) the seismicity rate r defined as the inverse of the duration of the window. For each function, we declare an alarm when the function is either larger (for M max and r) or smaller (for b) than a threshold. The quality of the predictions is measured by plotting the ratio of failures to predict as a function of the total durations of the alarms normalized by the duration of the catalog.